

Stochastic model of dispersive multi-step polarization switching in ferroelectrics due to spatial electric field distribution

R. Khachatryan,^{1, a)} J. Schultheiß,² J. Koruza,² and Y.A. Genenko^{1, b)}

¹⁾*Institut für Materialwissenschaft, Technische Universität Darmstadt, Otto-Berndt-Straße 3, D-64287 Darmstadt, Germany*

²⁾*Institut für Materialwissenschaft, Technische Universität Darmstadt, Alarich-Weiss-Straße 2, D-64287 Darmstadt, Germany*

(Dated: 5 August 2021)

A stochastic model for polarization switching in tetragonal ferroelectric ceramics is introduced, which includes sequential 90°- and parallel 180°-switching processes and accounts for the dispersion of characteristic switching times due to a nonuniform spatial distribution of the applied field. It presents merging of the recent multistep stochastic mechanism (MSM) with the earlier nucleation limited switching (NLS) and inhomogeneous field mechanism (IFM) models. The new model provides a much better description of simultaneous polarization and strain responses over a wide time window and a deeper insight into the microscopic switching mechanisms, as is exemplarily shown by comparison with measurements on lead zirconate titanate.

^{a)}Electronic address: rubenftf@gmail.com

^{b)}Electronic address: genenko@mm.tu-darmstadt.de

Multi-step non-180° polarization switching events were experimentally observed in ferroelectrics since the 90's by diffraction techniques¹⁻³, ultrasonic methods⁴, and microscopy^{5,6}. Although the account of these processes is ultimately necessary to describe the electromechanical response of ferroelectrics to an applied electric field, they are not included in common statistical models of polarization response, such as the Kolmogorov-Avrami-Ishibashi (KAI)⁷⁻¹⁰, the nucleation limited switching (NLS)¹¹⁻¹³ and the inhomogeneous field mechanism (IFM)¹⁴⁻¹⁶ models, dealing with statistically independent parallel 180° switching processes only. Furthermore, experimental results revealed that both 180° and non-180° switching events are required in order to describe the electrical and mechanical response of polycrystalline ceramics to an applied electric field pulse during polarization reversal¹⁷⁻¹⁹. Understanding of switching mechanisms and, particularly, knowing the fractions of 180° and non-180° contributions, is necessary for optimization of piezoelectric properties of materials^{20,21}. To this end, the fraction of non-180° switching events in a tetragonal BaTiO₃ at room temperature was evaluated to be around 20% by means of *in situ* X-ray diffraction²². Using the recently advanced multistep stochastic mechanism (MSM) model²³ for the analysis of simultaneous polarization and strain measurements, this fraction was found to be about 34% in a tetragonal lead zirconate titanate (Pb_{0.985}La_{0.01}(Zr_{0.475}Ti_{0.525})O₃) at room temperature.

A common difficulty for both experimental and theoretical statistical analysis consists in the possibility of hypothetical coherent non-180° processes, suggested by Arlt²⁴, which do not contribute to macroscopic strain and thus appear to be mechanically identical to the 180° reversal events. Another origin of uncertainty of interpretation of experimental results within the MSM model consists in the simplifying assumption of the uniform electric field all over the system. This assumption does not allow explanation of dispersive polarization and strain responses at later switching stages²³, which may result from the distribution of local switching times due to the spatially inhomogeneous distribution of the applied field^{14,15,25}. To account for this circumstance and to improve the description of the experiment²³, in the present study the NLS and the IFM models are merged with the MSM model. This means that both sequential 90°-and parallel 180°-switching processes are deemed to be driven by a nonuniformly distributed applied field. Similar to the previous KAI, NLS and IFM models, the actual hybrid model neglects electric and elastic interactions between the switching regions during polarization reversal.

In this model, a poled polycrystalline tetragonal ferroelectric is assumed to be uniformly

polarized in the negative z -direction, exhibiting a saturation polarization $-P_s$ (see Fig. 1(c)). When a reversed field is applied in the positive z -direction, the local polarization may experience two sequential 90° switching events (Fig. 1(a)) or a single 180° switching event (Fig. 1(b))¹⁹. The MSM model²³ describes the macroscopic polarization response Δp of this simplified system in z -direction by the formula

$$\begin{aligned} \frac{\Delta p(t)}{2P_s} = & \eta \left\{ 1 - \exp \left[- \left(\frac{t}{\tau_1} \right)^\alpha \right] \right\} - \frac{\eta}{2} L_1(t) \\ & + (1 - \eta) \left\{ 1 - \exp \left[- \left(\frac{t}{\tau_3} \right)^\gamma \right] \right\} \end{aligned} \quad (1)$$

with a convolution of the 90° events

$$L_1(t) = \int_0^t \frac{dt_1}{\tau_1} \alpha \left(\frac{t}{\tau_1} \right)^{\alpha-1} \exp \left[- \left(\frac{t_1}{\tau_1} \right)^\alpha - \left(\frac{t-t_1}{\tau_2} \right)^\beta \right] \quad (2)$$

where the parameter $\eta < 1$ quantifies the fraction of the 90° -switching events, τ_i are the unique characteristic switching times for the first and the second 90° -switching processes ($i = 1$ and 2 , respectively) and the parallel 180° - processes ($i = 3$), while α, β and γ are the Avrami indexes of the respective processes related to the dimensionality of the growing reversed polarization domains^{8,9}. According to Merz²⁶ and experimental observations on PZT ceramics^{12-15,19,23} the field dependence of the characteristic switching times is adopted in the form

$$\tau_i(E_a) = \tau_0 \exp \left(E_A^{(i)} / E_a \right) \quad (3)$$

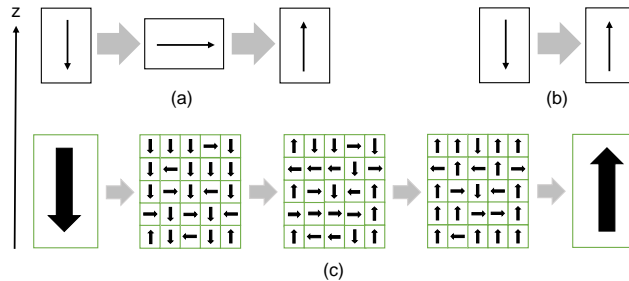


FIG. 1. Changes in polarization and geometry of a unit cell due to idealized (a) sequential 90° and (b) parallel 180° switching events. (c) Switching of a macroscopic sample by both types of events. Green boxes represent independently-switching regions.

where $E_A^{(i)}$ are the activation fields for the above mentioned switching processes, and E_a is the value of the applied uniform electric field. While in the framework of the MSM model regions of different length scales are assumed to switch statistically independent, this concept is able to account for the influence of microscopic parameters (*e.g.*, lattice inhomogenities, defects, chemical dopants) directly reflected in the determined characteristic switching times and activation fields.

The time-dependent change of the strain in z -direction is given in the MSM model by the formula

$$\Delta S_3(t) = \Delta S_{max} \eta L_1(t) + 2\varepsilon_0 \varepsilon_{33} Q_{11} E_a (\Delta p(t) - P_s) \quad (4)$$

with L_1 and Δp functions of time defined by Eqs. (2) and (1), respectively, ε_0 and ε_{33} the permittivity of vacuum and the relative permittivity in z -direction, respectively, and ΔS_{max} the maximum negative strain. Voigt notations²⁷ are used for the components of the strain tensor \mathbf{S} and the tensor of electrostriction \mathbf{Q} .

If now a nonuniform distribution of an applied electric field in a polycrystalline ceramic is taken into account, the local values E of the electric field become also strayed around the value E_a with some statistical distribution function $Z(E)$. Differently from the case of parallel switching processes^{15,16}, the latter function cannot be easily derived from the polarization response in the case of sequential processes. To keep the theory as simple as possible, the function $Z(E)$ may be assumed to have a Lorentzian form, as adopted by Jo *et al.* in the NLS model^{12,13}. Furthermore, due to scaling properties of the polarization response well established in PZT and other ceramics^{14,15,28-32}, it can be chosen in a scaling form with a dimensionless width of the field distribution κ :

$$Z(E) = \frac{1}{\pi E_a} \frac{\kappa}{(E/E_a - 1)^2 + \kappa^2}. \quad (5)$$

Introducing Eq. (5) in Eq. (1) an extended form results:

$$\begin{aligned} \frac{\Delta p(t)}{2P_s} = & \int_0^\infty dE Z(E) \left\{ \eta \left[1 - \exp \left(- \left(\frac{t}{\tau_1(E)} \right)^\alpha \right) \right] \right. \\ & \left. + (1 - \eta) \left[1 - \exp \left(- \left(\frac{t}{\tau_3(E)} \right)^\gamma \right) \right] \right\} - \frac{\eta}{2} L_1(t) \end{aligned} \quad (6)$$

with

$$\begin{aligned}
L_1(t) &= \int_0^t dt_1 \int_0^\infty dE_1 Z(E_1) \frac{\alpha}{\tau_1(E_1)} \left(\frac{t_1}{\tau_1(E_1)} \right)^{\alpha-1} \\
&\times \int_0^\infty dE_2 Z(E_2) \exp \left[- \left(\frac{t}{\tau_1(E_1)} \right)^\alpha - \left(\frac{t-t_1}{\tau_2(E_2)} \right)^\beta \right]
\end{aligned} \tag{7}$$

where E, E_1 and E_2 present local field values. For the strain response in this case the previous formula (4) still applies; however, with the functions $\Delta p(t)$ and $L_1(t)$ defined by Eqs. (6) and (7), respectively.

The formulas (4-7), from now on termed as the MSM-NLS approach, were used to fit simultaneous temporal measurements of polarization and strain response of $\text{Pb}_{0.985}\text{La}_{0.01}(\text{Zr}_{0.475}\text{Ti}_{0.525})\text{O}_3$ ceramic with tetragonal phase symmetry²³. We note that the only additional fitting parameter in comparison with Eqs. (1) and (2) of the MSM model was the field distribution width κ . The fitting results shown in Fig. 2 by solid lines for different applied fields are in much better agreement with experimental data, shown by symbols, than the previous calculations using the MSM model²³ neglecting the dispersive features of the response. The fitting parameters used in all shown graphs are $P_s = 0.38 \text{ C/m}^2$, $\Delta S_{max} = -1\%$, $\varepsilon_{33} = 2.85 \times 10^3$, $Q_{11} = 0.038 \text{ m}^4/\text{C}^2$, $\tau_0 = 0.8 \times 10^{-11} \text{ s}$, $\alpha = 0.28$, $\gamma = 2$, $\beta = 3$ for $E_a < 1.5 \text{ kV/mm}$ and 2 for $E_a > 1.5 \text{ kV/mm}$, $\eta = 0.42$, $\kappa = 0.012$, $E_A^{(1)} = 29 \text{ kV/mm}$, $E_A^{(2)} = 32.6 \text{ kV/mm}$, $E_A^{(3)} = 32.5 \text{ kV/mm}$. Macroscopic parameters are in reasonable agreement with independently measured polarization and strain characteristics²³. The determination of the microscopic fitting parameters has an inaccuracy below 1.3% for $\alpha, \beta, \gamma, \kappa$ and η , and below 0.5% for activation fields $E_A^{(i)}$. Note that the best fitting of experimental data was reached for the practically coinciding model parameters $E_A^{(2)}$ and $E_A^{(3)}$, followed by the coinciding characteristic times of the model τ_2 and τ_3 .

In spite of the satisfactory description of the experiment by the formulas (4-7) they contain triple integration and are rather cumbersome for data fitting. In a more simple approach, conceptually closer to the previous IFM model^{14,15}, the local switching processes characterized by Avrami indexes larger than 2 can be substituted by step-functions on the logarithmic time scale¹⁵ allowing for explicit integration over the local field variables in

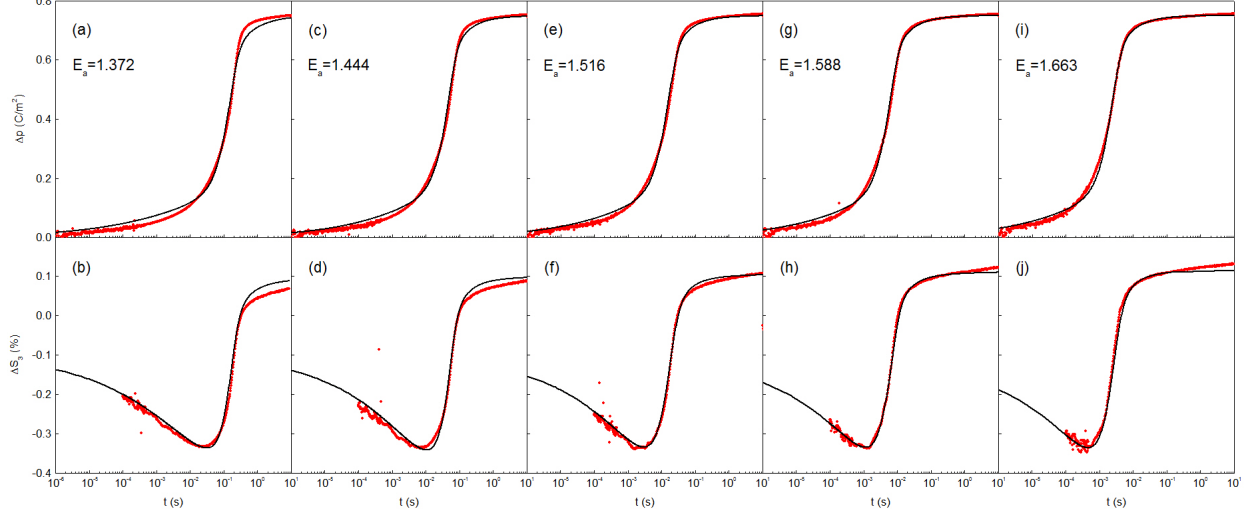


FIG. 2. Simultaneous variation of the polarization (a), (c), (e), (g), (i) and strain (b), (d), (f), (h), (j) with time at different field values in kV/mm as indicated in the plots. Experimental curves are shown by red symbols and fitting by means of the MSM-NLS model by black solid lines.

Eqs. (4-7). This results in a simpler form, from now on termed as the MSM-IFM model,

$$\begin{aligned}
\Delta p(t) = & 2P_s\eta \left\{ 1 - \exp \left[- \left(\frac{t}{\tau_1} \right)^\alpha \right] \right\} \\
& + 2P_s(1 - \eta) \left\{ \frac{1}{2} + \frac{1}{\pi} \arctan \left[\ln \left(\frac{t}{t_3} \right) / W_3 \right] \right\} \\
& - P_s\eta \frac{\alpha}{\tau_1} \int_0^t dt_1 \left(\frac{t_1}{\tau_1} \right)^{\alpha-1} \exp \left[- \left(\frac{t_1}{\tau_1} \right)^\alpha \right] \\
& \times \left\{ \frac{1}{2} - \frac{1}{\pi} \arctan \left[\ln \left(\frac{t-t_1}{t_2} \right) / W_2 \right] \right\}. \tag{8}
\end{aligned}$$

containing only one integration over the intermediate moment t_1 , which is unavoidable when describing the convolution of two sequential switching events. Here, the ansatz $\tau_1 = \tau_0 \exp \left(E_A^{(1)} / E_a \right)$ is retained while the characteristic times t_2 and t_3 are assumed equal to each other together with their activation fields,

$$t_{2,3} = \tau_0 \exp \left(\frac{E_A^{(2)}}{E_a(1 + \kappa^2)} \right) \text{ and } W_{2,3} = \frac{\kappa}{1 + \kappa^2} \frac{E_A^{(2)}}{E_a}, \tag{9}$$

according to the above fitting of the experimental data by the MSM-NLS model. The resulting description of the experiment shown in Fig. 3 appears to be of inferior quality to that of the MSM-NLS model, shown in Fig. 2, however, the simpler MSM-IFM model also

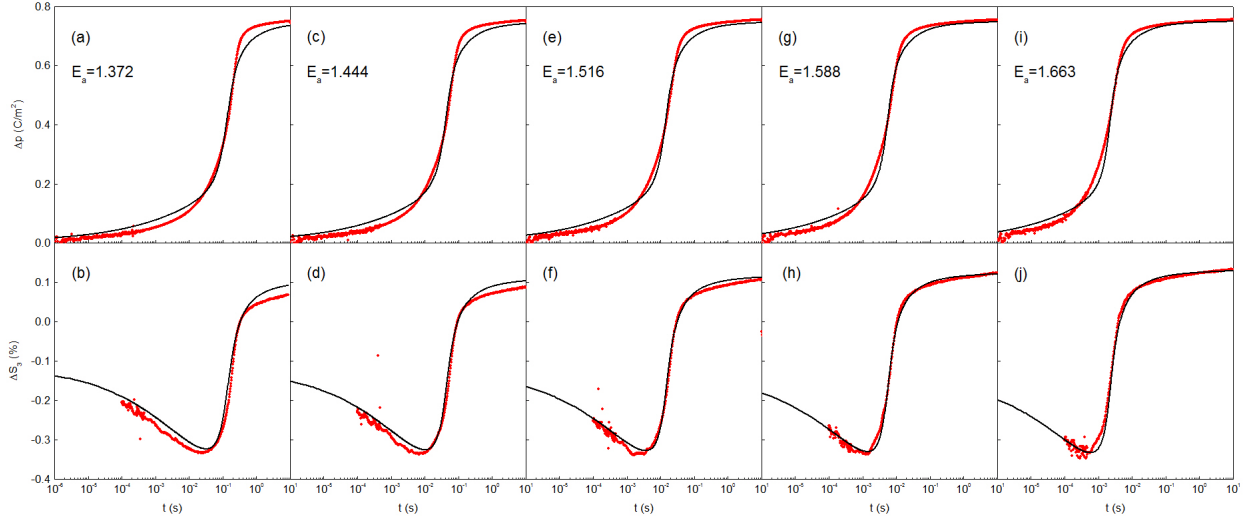


FIG. 3. Simultaneous variation of the polarization (a), (c), (e), (g), (i) and strain (b), (d), (f), (h), (j) with time at different field values in kV/mm as indicated in the plots. Experimental curves are shown by red symbols and fitting by means of the MSM-IFM model by black solid lines.

well describes the main features of polarization and strain kinetics, especially at high fields. Several parameters of the model thereby get somewhat modified, namely, $E_A^{(2)} = E_A^{(3)} = 32.4$ kV/mm, $\eta = 0.40$, $Q_{11} = 0.044$ m⁴/C², $\kappa = 0.023$. The fair quality of the fitting may result from the relatively narrow field distribution function, Eq. (5), which limits the validity of the used step-function approximation²³. It is expected that the performance of the MSM-IFM approach will be better for systems with broader field distributions.

Introduction of the statistical distribution of local field values remarkably improved the description of the electromechanical response, as compared with the MSM model²³ assuming the uniform electric field. The dispersion of the field values and, consequently, of the local switching times, has the highest impact on the later stage of switching. However, particularly this switching stage with a quasilinear behavior on the logarithmic time scale in Figs. 2 and 3 is still not always properly captured by the both MSM-NLS and MSM-IFM models, especially at low applied fields. It was suggested that this stage may appear due to a long-time electromechanical creep of the domain structure^{19,33}. It is known, on the other hand, that such time dependences typically occur due to asymmetric field distributions enhanced in the low field region^{14,28,30–32}, the feature missing here because of the simplifying choice of the symmetric Lorentzian distribution, Eq. (5). Using more realistic asymmetric field

distributions may improve the performance of both models in the low field region.

Concerning the switching times governed by the respective activation fields, the considerably shorter switching times $\tau_1(E_a)$ and the smallest activation field $E_A^{(1)}$ of the first 90°-switching processes are probably due to mechanical support by release of residual stresses, as suggested by Daniels *et al.*³. Furthermore, we note an astounding fact of the virtually identical activation fields $E_A^{(2)}$ and $E_A^{(3)}$ attributed to the presumably physically different – 90° and 180° – switching processes which are characterized by rather different activation energies³⁴. This coincidence may be related to the hypothesis by Arlt²⁴, who suggested a possible scenario of the coherent 90° switching events, which do not contribute to the spontaneous strain, but contribute to the polarization and thus may be experimentally mistaken for 180° processes. For this to occur, these processes should be correlated over mesoscopic length scales depending on the microstructural properties of materials. We note that the formulas (1,2,6,7,8) do not assume explicitly, but also do not preclude, correlated switching processes. Generally, atomistic³⁴ simulations in uniform media are strongly in favor of highly correlated 90° switching processes, coherent over macroscopic scales, which is confirmed by direct optical observations on a BaTiO₃ single crystal³⁵. Macroscopically coherent switching is also predicted by other atomistic³⁶ and phase-field³⁷ simulations for single crystals. The study of correlations in the polarization response of thin ferroelectric films revealed coherent behavior of up to 1000 grains^{38,39} which, however, may be mediated by elastic coupling through the substrate^{40,41}. Switching processes in bulk ceramics seem to be rather correlated at a short-range scale involving around 20 grains^{42,43} which roughly corresponds to the number of the next neighbors. Similar conclusions on the correlation length scale were derived from 2D⁴⁴ and 3D⁴⁵ simulations where, however, only electric interactions were taken into account. Polarization correlations of neighboring grains due to domains crossing grain boundaries were observed by optical observations⁴⁶, TEM and PFM⁴⁷.

In conclusion, by supplementing the recent multistep stochastic mechanism (MSM) model of polarization switching in ferroelectrics²³ with the statistical distribution of local electric fields, the new hybrid MSM-NLS model (with its simplified MSM-IFM version) was advanced. The new model allows description of the simultaneous polarization and strain response of ferroelectric ceramics over a wide time domain with high accuracy that was exemplarily shown for a tetragonal PZT ceramic. Particularly, it allows determination of the fractions of sequential 90°- and parallel 180°-switching events η . However, the analysis of

the model parameters resulting from the fitting of experiments revealed a notable fact that the switching time and activation field for the second sequential 90°-switching processes coincide with those of the parallel 180°-switching events. The contribution of the latter into polarization and strain can hardly be distinguished from such coherent 90°-switching processes, which do not contribute to the spontaneous strain²⁴. Though the present model, as well as other common statistical models, are based on the assumption of statistically-independent switching events, the coincidence of the switching times and activation fields of the sequential 90°- and parallel 180°-switching processes can hardly be accidental. This might indicate that the polarization reversal is rather dominated by a mix of statistically independent and coherent 90°-switching events, correlated on different length-scales within and beyond the grains, than by parallel 180°-switching events.

This work was supported by the Deutsche Forschungsgemeinschaft (DFG) Grants No. GE 1171/7-1 and No. KO 5100/1-1.

REFERENCES

- ¹S. P. Li, A. S. Bhalla, R. E. Newnham, L. E. Cross, and C. Y. Huang, *J. Mater. Sci.* **29**, 1290 (1994).
- ²J. E. Daniels, T. R. Finlayson, M. Davis, D. Damjanovic, A. J. Studer, M. Hoffman, and J. L. Jones, *J. Appl. Phys.* **101**, 104108 (2007).
- ³J. E. Daniels, C. Cozzan, S. Ukritnukun, G. Tutuncu, J. Andrieux, J. Glaum, C. Dosch, W. Jo, and J. L. Jones, *J. Appl. Phys.* **115**, 224104 (2014).
- ⁴J. Yin and W. Cao, *Appl. Phys. Lett.* **79**, 4556 (2001).
- ⁵C. Y. Hsieh, Y. F. Chen, W. Y. Shih, Q. Zhu, and W. H. Shih, *Appl. Phys. Lett.* **94**, 131101 (2009).
- ⁶R. Xu, S. Liu, I. Grinberg, J. Karthik, A.R. Damodaran, A.M. Rappe, L.W. Martin, *Nat. Mater.* **14**, 79 (2015).
- ⁷A. Kolmogoroff, *Izv. Akad. Nauk SSSR, Ser. Mat.* **1**, 355 (1937).
- ⁸M. Avrami, *J. Chem. Phys.* **8**, 212 (1940).
- ⁹Y. Isibashi and Y. Takagi, *J. Phys. Soc. Japan* **31**, 506 (1971).

- ¹⁰H. Orihara, S. Hashimoto, and Y. Isibashi, *J. Phys. Soc. Japan* **63**, 1031 (1994).
- ¹¹A. K. Tagantsev, I. Stolichnov, N. Setter, J. S. Cross, M. Tsukada, *Phys. Rev. B* **66**, 214109 (2002).
- ¹²J. Y. Jo, H. S. Han, J.-G. Yoon, T. K. Song, S.-H. Kim, T. W. Noh, *Phys. Rev. Lett.* **99**, 267602 (2007).
- ¹³J. Y. Jo, S. M. Yang, H. S. Han, D. J. Kim, W. S. Choi, T. W. Noh, T. K. Song, J.-G. Yoon, C. Y. Koo, J.-H. Cheon, and S.-H. Kim, *Appl. Phys. Lett.* **92**, 012917 (2008).
- ¹⁴S. Zhukov, Y. A. Genenko, O. Hirsch, J. Glaum, T. Granzow, and H. von Seggern, *Phys. Rev. B* **82**, 014109 (2010).
- ¹⁵Y. A. Genenko, S. Zhukov, S. V. Yampolskii, J. Schüttrumpf, R. Dittmer, W. Jo, H. Kungl, M. J. Hoffmann, and H. von Seggern, *Adv. Funct. Mater.* **22**, 2058 (2012).
- ¹⁶J. Lee, A. J. J. M. van Breemen, V. Khikhlovskiy, M. Kemerink, R. A. J. Janssen, and G. H. Gelinck, *Sci. Rep.* **6**, 24407 (2016).
- ¹⁷A. Yamada, Y.-K. Chung, M. Takahashi, and T. Ogawa, *Jap. J. Appl. Phys.* **35**, 5232 (1996).
- ¹⁸T. Ogawa and K. Nakamura, *Jap. J. Appl. Phys.* **37**, 5241 (1998).
- ¹⁹J. Schultheiß, L. Liu, H. Kungl, M. Weber, L. Kodumudi Venkataraman, S. Checchia, D. Damjanovic, J. E. Daniels, J. Koruza, *Acta Mater.* **157**, 355 (2018).
- ²⁰A. Pramanick, D. Damjanovic, J. E. Daniels, J. C. Nino, and J. L. Jones, *J. Am. Ceram. Soc.* **94**, 293 (2011).
- ²¹J. Glaum, Y. A. Genenko, H. Kungl, L. A. Schmitt, and T. Granzow, *J. Appl. Phys.* **112**, 034103 (2012).
- ²²C. M. Fancher, S. Brewer, C. C. Chung, S. Rohrig, T. Rojac, G. Esteves, M. Deluca, N. Bassiri-Gharb, and J. L. Jones, *Acta Mater.* **126**, 36 (2017).
- ²³Y. A. Genenko, R. Khachatryan, J. Schultheiß, A. Ossipov, J. E. Daniels, and J. Koruza, *Phys. Rev. B* **97**, 144101 (2018).
- ²⁴G. Arlt, *Integr. Ferroelectr.* **16**, 229 (1997).
- ²⁵D. C. Lupascu, S. Fedosov, C. Verdier, J. Rödel, and H. von Seggern, *J. Appl. Phys.* **95**, 1386 (2004).
- ²⁶W. J. Merz, *J. Appl. Phys.* **27**, 938 (1956).
- ²⁷R. E. Newnham, *Properties of Materials. Anisotropy, Symmetry, Structure* (Oxford University Press Inc., New York, 2005).

- ²⁸S. Zhukov, Y. A. Genenko, M. Acosta, H. Humburg, W. Jo, J. Rödel, and H. von Seggern, *Appl. Phys. Lett.* **103**, 152904 (2013).
- ²⁹S. Zhukov, H. Kungl, Y. A. Genenko, and H. von Seggern, *J. Appl. Phys.* **115**, 014103 (2014).
- ³⁰S. Zhukov, M. Acosta, Y. A. Genenko, and H. von Seggern, *J. Appl. Phys.* **118**, 134104 (2015).
- ³¹S. Zhukov, J. Glaum, H. Kungl, E. Sapper, R. Dittmer, Y. A. Genenko, and H. von Seggern, *J. Appl. Phys.* **120**, 064103 (2016).
- ³²S. Zhukov, Y. A. Genenko, J. Koruza, J. Schultheiß, H. von Seggern, W. Sakamoto, H. Ichikawa, T. Murata, K. Hayashi, and T. Yogo, *Appl. Phys. Lett.* **108**, 012907 (2016).
- ³³Q. D. Liu and J. E. Huber, *J. Eur. Ceram. Soc.* **26**, 2799 (2006).
- ³⁴S. Liu, I. Grinberg and A. M. Rappe, *Nature* **534**, 360 (2016).
- ³⁵B. Jiang, Y. Bai, W. Chu, Y. Su, and L. Qiaob, *Appl. Phys. Lett.* **93**, 152905 (2008).
- ³⁶A. Leschhorn and H. Kliem, *J. Appl. Phys.* **121**, 014103 (2017).
- ³⁷J. E. Zhou, T.-L. Cheng, and Y. U. Wang, *J. Appl. Phys.* **111**, 024105 (2012).
- ³⁸P. Bintachitt, S. Trolier-McKinstry, K. Seal, S. Jesse, and S. V. Kalinin, *Appl. Phys. Lett.* **94**, 042906 (2009).
- ³⁹K. Seal, S. Jesse, M. P. Nikiforov, S. V. Kalinin, I. Fujii, P. Bintachitt, and S. Trolier-McKinstry, *Phys. Rev. Lett.* **103**, 057601 (2009).
- ⁴⁰P. Bintachitt, S. Jesse, D. Damjanovic, Y. Han, I. M. Reaney, S. Trolier-McKinstry, and S. V. Kalinin, *Proc. Natl. Acad. Sci. USA* **107**, 7219 (2010).
- ⁴¹F. Griggio, S. Jesse, A. Kumar, O. Ovchinnikov, H. Kim, T. N. Jackson, D. Damjanovic, S. V. Kalinin, and S. Trolier-McKinstry, *Phys. Rev. Lett.* **108**, 157604 (2012).
- ⁴²J. E. Daniels, M. Majkut, Q. Cao, S. Schmidt, J. Wright, W. Jo, and J. Oddershede, *Sci. Rep.* **6**, 22820 (2016).
- ⁴³M. Majkut, J. E. Daniels, J. P. Wright, S. Schmidt, and J. Oddershede, *J. Am. Ceram. Soc.* **100**, 393 (2017).
- ⁴⁴R. Khachatryan, J. Wehner and Y. A. Genenko, *Phys. Rev. B* **96**, 054113 (2017).
- ⁴⁵R. Khachatryan and Y. A. Genenko, *Phys. Rev. B* **98**, 134106 (2018).
- ⁴⁶R. C. Devries and J. E. Burke, *J. Amer. Ceram. Soc.* **40**, 200 (1957).
- ⁴⁷D. M. Marincel , H. Zhang, A. Kumar, S. Jesse, S. V. Kalinin, W. M. Rainforth, I. M. Reaney, C. A. Randall, and S. Trolier-McKinstry, *Adv. Funct. Mater.* **24**, 1409 (2014).